

Longitudinal Dynamics of Electrons in the Femtosource Without Beam Current Effects

Alexander Zholents

Recall, that our initial thoughts for a longitudinal dynamic of the electron beam in the femtosource were as follows. We considered a system where a 10 ps electron bunch (total width, uniform distribution) produced in the photocathode was accelerated to approximately 120 MeV, compressed to 5 ps, accelerated more to 2.5 GeV and finally compressed to 1 ps. However, the present analysis of this scheme shows that the compression of 5 ps electron bunch at 2.5 GeV is not a good idea. We were not able to compress the electron bunch even to 2 ps (not 1 ps) without the excessive growth of the beam energy spread (several times more than it was initially expected). Presently, we also consider longer than 10 ps electron bunch from the photocathode gun (20 ps or even 40 ps) to get better transverse emittance. Obviously it will make the execution of our initial scheme of the electron bunch compression much more difficult, if possible at all.

Therefore, we consider a new scheme which does all bunch compression in the injector part of the machine. We also consider to limit the compression to 2 ps rather than 1 ps in order to mitigate possible CSR effects in the arcs during the acceleration in the recirculating linac. As we understood from a preliminary analysis of the x-ray compression, it will not compromise obtaining 60-70 fs x-ray pulses.

Our new scheme consists of the following chain of the linear accelerators and bunch compressors. We begin with the acceleration of the electron bunch in the photocathode gun to 10 MeV. In this note we assume that the acceleration there takes place on the crest of the RF wave, although other phases can be treated equally. Then we use third harmonic linearizer (3.9 GHz cavity) followed by the bunch compressor. Then we use the injector linear accelerator to bring electron energy to 120 MeV and the second linearizer. Then we compress the electron bunch to 2 ps in the 180° injection arc. Finally, we accelerate electrons in the recirculating linac to 2.5 GeV. We assume that all arcs in the recirculator are isochronous.

10 ps electron bunch

In the following plots below we show the evolution of the longitudinal phase space of the electron bunch as it progresses down the chain of the transformations. We begin with the window-frame distribution shown in Figure 1, where border lines are set at ± 10 ps and ± 20 keV. This is assumed to be the border lines for our longitudinal emittance coming out of the photocathode gun.

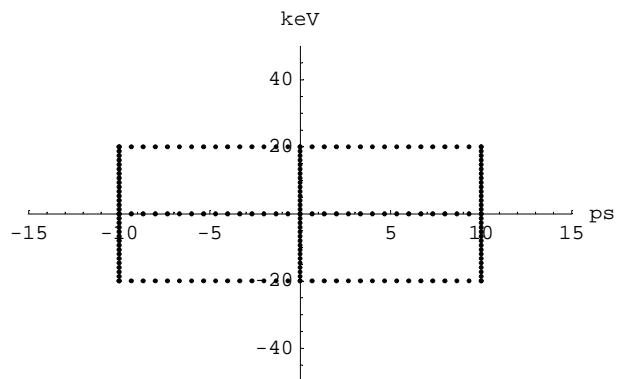


Figure 1. The initial launch of the particles.

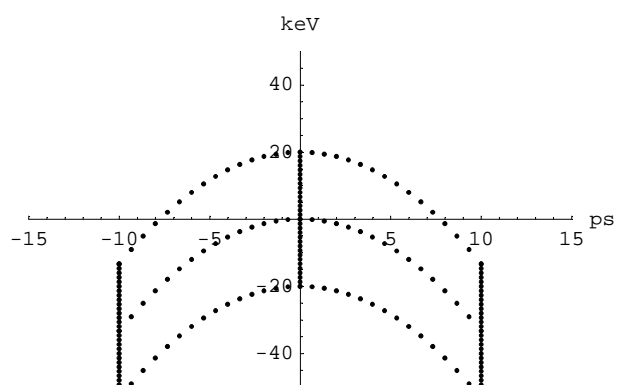


Figure 2. At the exit of the photocathode gun after acceleration to 10 MeV at the crest of the RF waveform (0° phase).

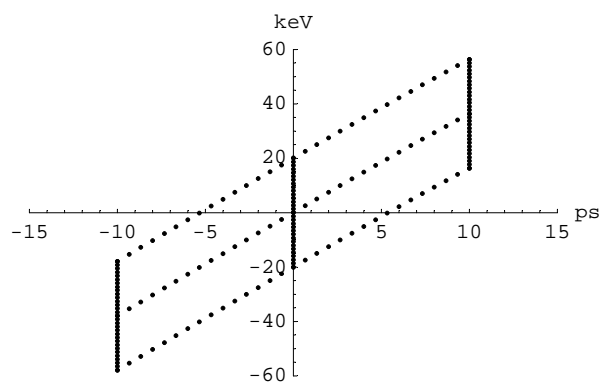


Figure 3. After the first linearizer: frequency=3.9 GHz, peak voltage=-1.1 MV, RF phase= 8° .

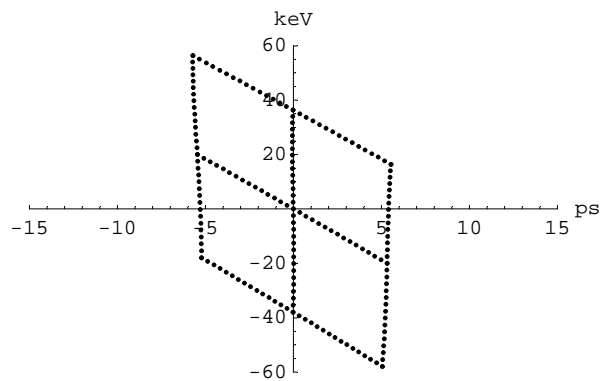


Figure 4. After the first bunch compressor. Time-of-flight matrix coefficients are: $R56=-0.76$ m, $T566=-4$ m.

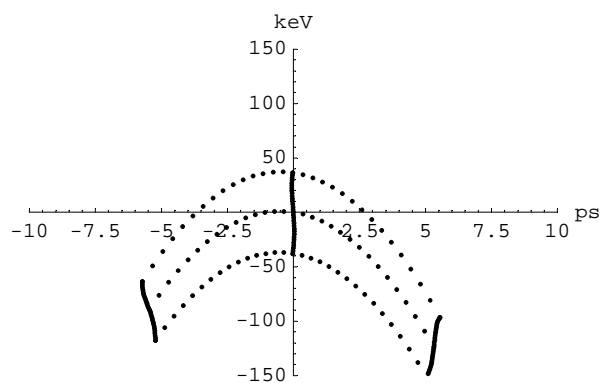


Figure 5. After the acceleration to 120 MeV in the injector linac at the crest of the RF waveform.

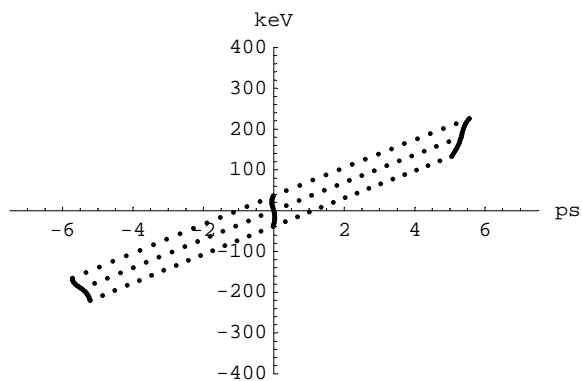


Figure 6. After the second linearizer: frequency=3.9 GHz, peak voltage=-12 MV, RF phase= 7.5° .

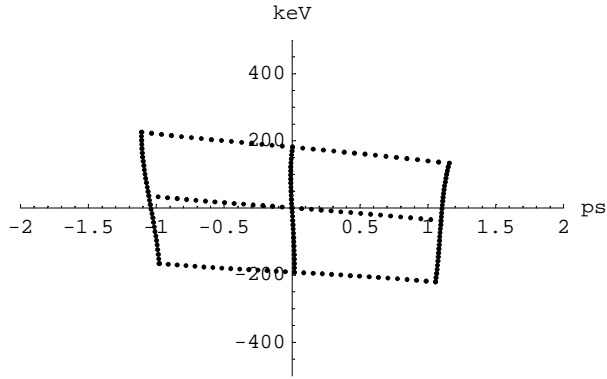


Figure 7. After the second bunch compression in the injection arc. Time-of-flight matrix coefficients are: $R56 = -0.93$ m, $T566 = -8$ m.

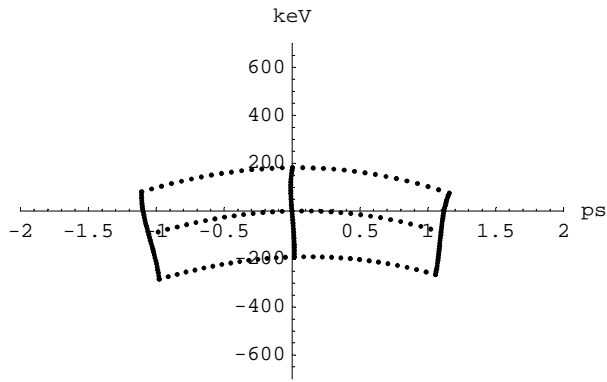


Figure 8. After the acceleration to 2.5 GeV in the recirculating linac at the crest of the RF waveform for the first three passes and at -0.5° phase at the last pass.

Next we pass the electron beam through the RF deflection cavity operated at 3.9 GHz at 90° phase from the crest. The following plot shows the tilt angle obtained by the electrons in the undulator as a function of the longitudinal off-set.

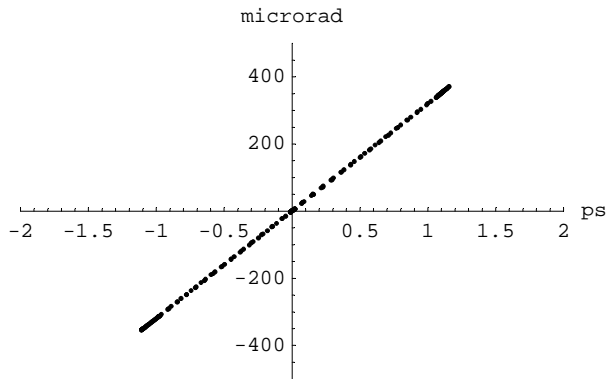


Figure 9. After the RF deflection: 3.9 GHz, 90° phase.

20 ps electron bunch

Now we use the same scheme to demonstrate the compression of 40 ps electron bunch. We assume that a two times increased bunch length is complemented by a two times decreased energy spread. Therefore, we launch particles on the window-frame with lines at ± 20 ps and ± 10 keV (see Figure 10).

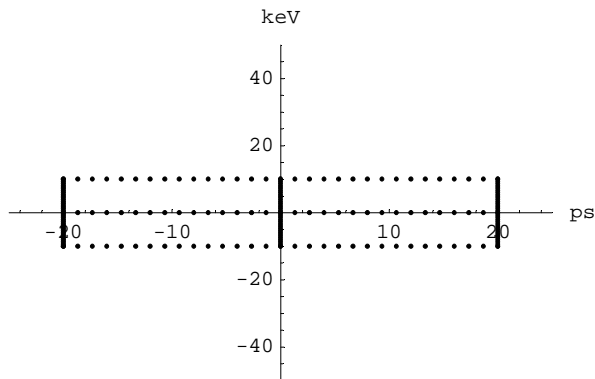


Figure 10. The initial launch of the particles.

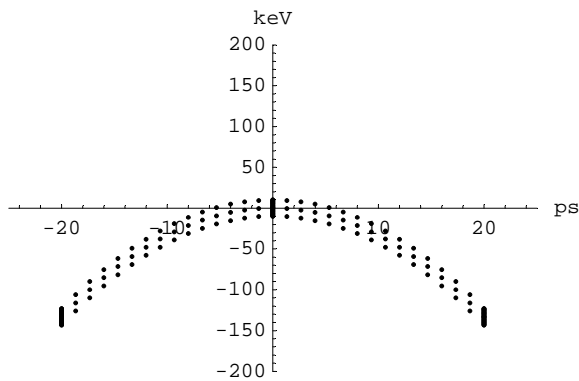


Figure 11. At the exit of the photocathode gun after acceleration to 10 MeV at the crest of the RF waveform (0° phase).

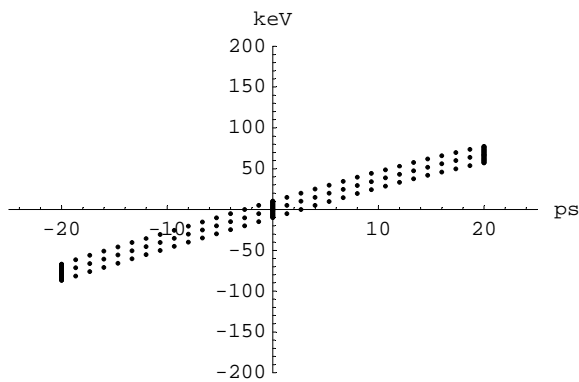


Figure 12. After the first linearizer: frequency=3.9 GHz, peak voltage=-1.1 MV, RF phase= 8° .

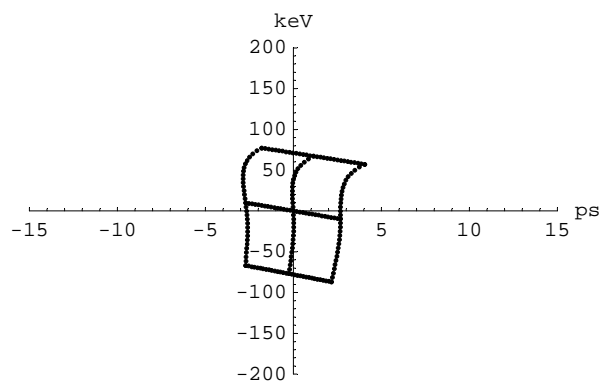


Figure 13. After the first bunch compressor. Time-of-flight matrix coefficients are: $R56 = -0.72$ m, $T566 = -4$ m.

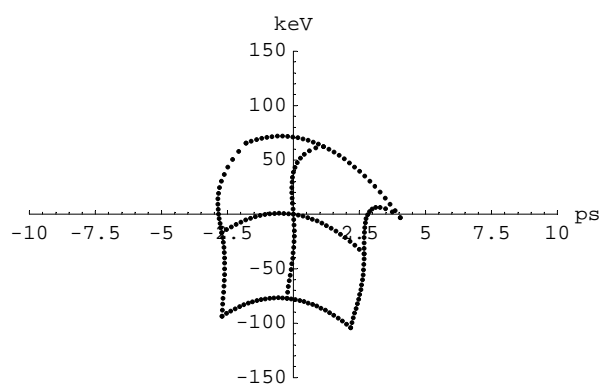


Figure 14. After the acceleration to 120 MeV in the injector linac at the crest of the RF waveform.

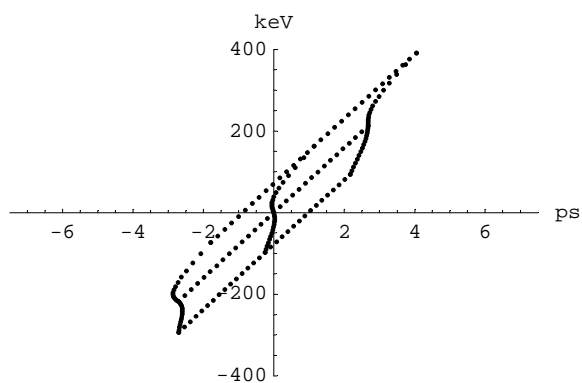


Figure 15. After the second linearizer: frequency=3.9 GHz, peak voltage=-12 MV, RF phase= 16° (recall, it was 7.5° in the 10 ps case).

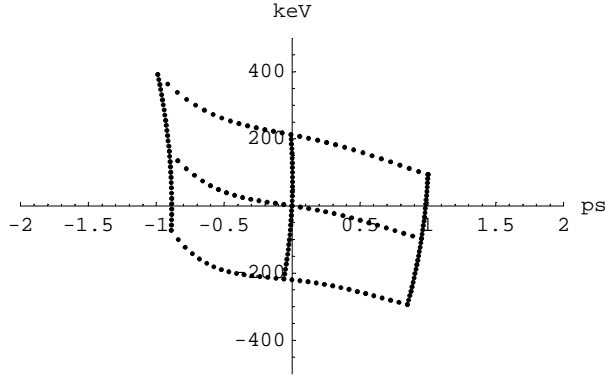


Figure 16. After the second bunch compression in the injection arc. Time-of-flight matrix coefficients are: $R56 = -0.40$ m, $T566 = -4$ m ($R56 = -0.93$ m, $T566 = -8$ m in the 10 ps case).

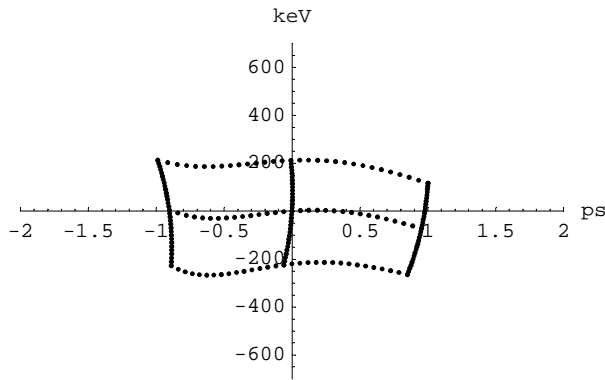


Figure 17. After the acceleration to 2.5 GeV in the recirculating linac at the crest of the RF waveform for the first three passes and at -1.2° phase at the last pass (-0.5° in the 10 ps case).

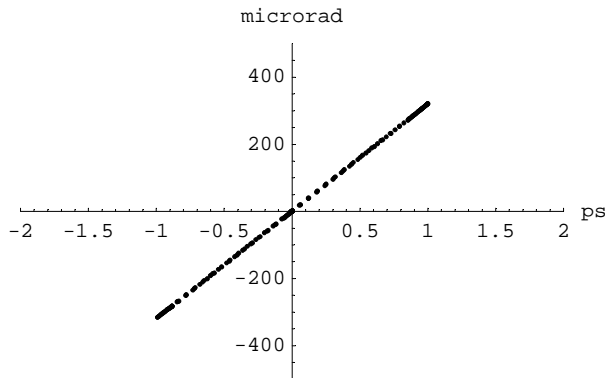


Figure 18. After the RF deflection: 3.9 GHz, 90° phase.

Comparing plots in Figures 17,18 with plots in Figures 8,9 we conclude that the increase of the bunch length to 20 ps can be accommodated in a new scheme.